

We are IntechOpen, the world's leading publisher of Open Access books Built by scientists, for scientists

6,900

Open access books available

186,000

International authors and editors

200M

Downloads

Our authors are among the

154

Countries delivered to

TOP 1%

most cited scientists

12.2%

Contributors from top 500 universities



WEB OF SCIENCE™

Selection of our books indexed in the Book Citation Index
in Web of Science™ Core Collection (BKCI)

Interested in publishing with us?
Contact book.department@intechopen.com

Numbers displayed above are based on latest data collected.
For more information visit www.intechopen.com



Undeniable Contribution of Aprotic Room Temperature Ionic Liquids in the Security of Li-Ion Batteries

Claude-Montigny Bénédicte, Stefan Claudia Simona and Violleau David
*Université François Rabelais, Laboratoire PCMB
France*

1. Introduction

Nowadays, lithium-ion batteries are key components for portable electric devices for applications between 0°C and 50°C. Between the positive electrode and the negative one of the Li-ion battery, the transport of the Li⁺ ions is insured by the electrolyte. Whatever the physical state of the electrolyte (liquid, polymer or gel), the direction of the transport stays the same: the Li⁺ ion passes from the positive pole towards the negative one during the charging process, and conversely during the discharge. Up to now, electrolytes most commonly used in Li-ion batteries present in their formulation one or several aprotic and polar organic solvents, mixed with a lithium salt and some additives. Typical liquid electrolytes are based on a mixture of cyclic or linear alkylcarbonates. These solvents are perfectly adapted to the functioning of batteries Li-ion, but they are volatile and highly flammable (Aurbach et al. 2004; MacNeil et al., 1999, 2000; MacNeil & Dahn, 2001; Rasch et al. 1991; Richard & Dahn, 1999). If the temperature of the battery overtakes 60-70°C, the slightest warm-up or the internal short circuit can thus induce a thermal racing, leading to an inflammation (Balakrishnan et al., 2006; Zhang, 2006). It is well also known that over 50°C, cycle life and capacity of lithium-ion batteries based on usual alkylcarbonate mixtures may be drastically reduced. They are still not well adapted for other applications, such as security lighting, portable sensors, geothermal energy, drillings and explorations of potential hydrocarbon deposits, lithium batteries which have to operate at higher temperatures than 50°C. High energy density Li-ion batteries present usually a very short life over 60°C. Polymer electrolytes should be more convenient at high temperature either in the form of solid polymer electrolyte or polymer gel electrolyte. Nevertheless solid polymer Li-ion batteries have relatively low ionic conductivities as compared to gel polymer electrolytes (Kobayashi et al., 2007). Unfortunately gel electrolytes are unstable above 80°C (Kaneko et al., 2009; Shin & Cairns, 2008). Therefore, in order to enhance the conductivity of the electrolyte and simultaneously to get free of the flammability of organic solvents, ionic liquids (ILs) appear to be a good solution for use as electrolyte in large scale Li-ion batteries. ILs present a flame resistance, a low volatility (no OVCs), and a large electrochemical stability (Lewandowski & Galinski, 2004; Wasserscheid & Welton, 2008). In particular, room temperature ionic liquids (RTILs), which are liquid at ambient or sub-ambient temperature, look suitable for the replacement of organic solvents or their mixtures (Appetecchi et al.,

2008; Kobayashi et al., 2007, Lall-Ramnarine et al., 2008; Nokemann et al., 2008). N-alkyl-N-alkyl' pyrrolidinium bis(trifluoromethylsulfonyl)imide RTILs are chosen for this use. These RTIL compounds present a high thermal stability (up to 300°C), low flammability and low glass transition temperatures (Pan et al., 2010; Wasserscheid & Welton, 2008). All these characteristics make them good candidates as electrolytes for electrochemical devices as long as their conductivity remains high in the range of operating temperatures. The purpose of this chapter concerns the use of a series of N-alkyl-N-alkyl' pyrrolidinium bis(trifluoromethylsulfonyl)imide RTILs (P_{xy} -TFSI, presented in Table 1) as co-solvents in the formulation of a standard electrolyte (PC (propylene carbonate)/EC (ethylene carbonate)/DMC (dimethyl carbonate) (1:1:3 w/w) + $LiPF_6$ (lithium hexafluorophosphate) 1M + VC (vinylene carbonate) 1 %).

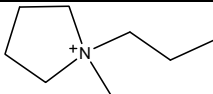
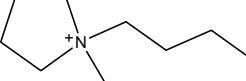
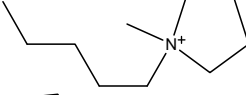
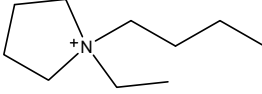
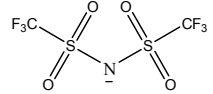
component	formula	abbreviation
N-methyl-N-propyl-pyrrolidinium		P_{13}^+
N-butyl-N-methyl-pyrrolidinium		P_{14}^+
N-methyl-N-pentyl-pyrrolidinium		P_{15}^+
N-butyl-N-ethyl-pyrrolidinium		P_{24}^+
bis(trifluoromethanesulfonyl)imide		TFSI ⁻

Table 1. Names, formula and abbreviations of N-alkyl-N-alkyl' pyrrolidinium imide (P_{xy} -TFSI) under study.

Thanks to the exceptional fire break property of this class of RTILs (Wasserscheid & Welton, 2008), an improvement in the security of Li-ion batteries is expected, without changing the electrochemical performances of the well known $LiCoO_2$ cathode and a graphite negative electrode compared to the standard electrolyte. The first part of this chapter concerns the tests of thermal stability and the flammability of electrolytes based on N-alkyl-N-alkyl' pyrrolidinium bis(trifluoromethylsulfonyl)imide RTILs (from Solvionic, Toulouse, France), added to the standard electrolyte. A second part will be dedicated to the transport properties of electrolytes containing these RTILs as co-solvents. These properties are highly dependent on ionic conduction in these media. A third part will be devoted to the wettability of both electrodes and separators in the presence of these RTILs. Indeed, the wettability is another key factor for improving the cycling ability and the power of Li-ion batteries, especially when the temperature decreases. This chapter will end by an electrochemical study using these mixtures as electrolytes, leading to capacity determination.

2. Thermal stability of the mixed electrolytes: P_{xy} -TFSI / standard electrolyte

The study of the thermal stability of the mixed electrolytes (standard electrolyte/RTIL) is performed at sub ambient temperatures as a function of the alkyl chain length of the P_{xy} -

TFSI RTIL in the mixture. The effect of the RTIL content on the thermal stability is also studied. Finally this study is completed by the results of the flammability tests of the analyzed mixtures, according to the added RTIL content.

2.1 Thermal analysis at sub-ambient temperatures: effect of the P_{xy}-TFSI nature and of its content

Samples containing mixtures of standard electrolyte with P_{xy}-TFSI RTIL, which content is 20% (w/w), are analyzed by differential scanning calorimetry, DSC, between 20°C and 400°C at the fixed scanning rate of 5°C/min for both the heating and the cooling steps. The resulting thermograms are displayed in the Figure 1 and Table 2. The phenomenon of vaporization is well identified on each of them by the existence of an endothermic corresponding peak during the heating step at 139°C for 20% P₁₃-TFSI, 174°C for 20% P₁₄-TFSI and at 203°C for 20% P₂₄-TFSI. During the cooling step, no thermal phenomenon is observed, that means that vapours are not able to be condensed (capsules containing the analyzed products opened, letting escape the vapours of solvents). The results, obtained by DSC under the same analysing conditions, for samples containing 30% of RTIL in the standard electrolyte, are reported in Table 2. The DSC thermograms bring to light peaks of vaporisation at 140°C for 30% P₁₃-TFSI, at 195°C for 30% P₁₄-TFSI, at 224°C for 30% P₁₅-TFSI. These values are thus globally a little higher than those of the mixtures containing 20% of P_{xy}-TFSI. For both contents, the vaporisation temperatures are higher than the DMC boiling point reported in Table 3. Except for the P₁₃-TFSI, all the mixtures (RTIL/standard electrolyte) present higher vaporisation temperature than the EC/PC/3DMC mixture and the pure VC solvent.

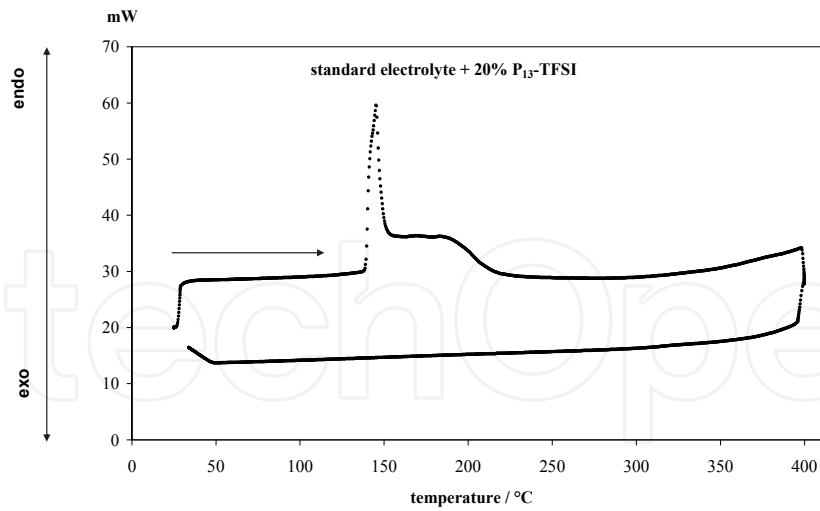
	P ₁₃ -TFSI		P ₁₄ -TFSI		P ₁₅ -TFSI	
	20%	30%	20%	30%	20%	30%
T _{vap.} / °C	139	140	174	195	203	224

Table 2. Temperatures of vaporization of various mixtures P_{xy}-TFSI/standard electrolyte.

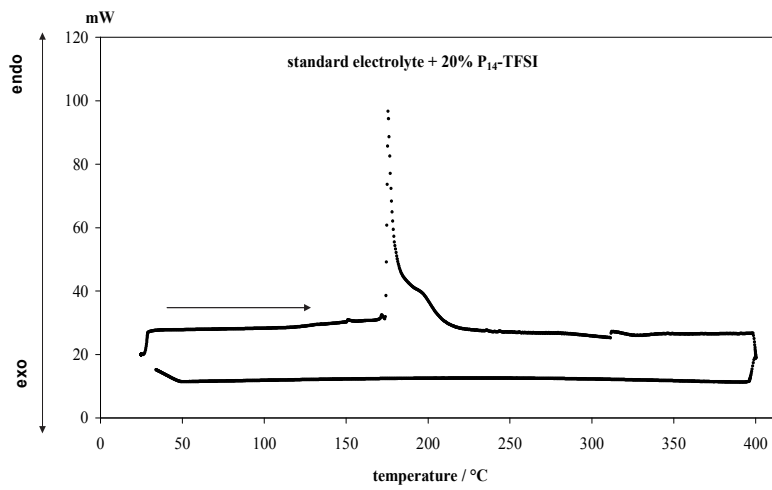
	PC	EC	DMC	VC	EC/PC/3DMC
Boiling point / °C	242	248	90	162	160

Table 3. DSC boiling points of the solvents composing the standard electrolyte.

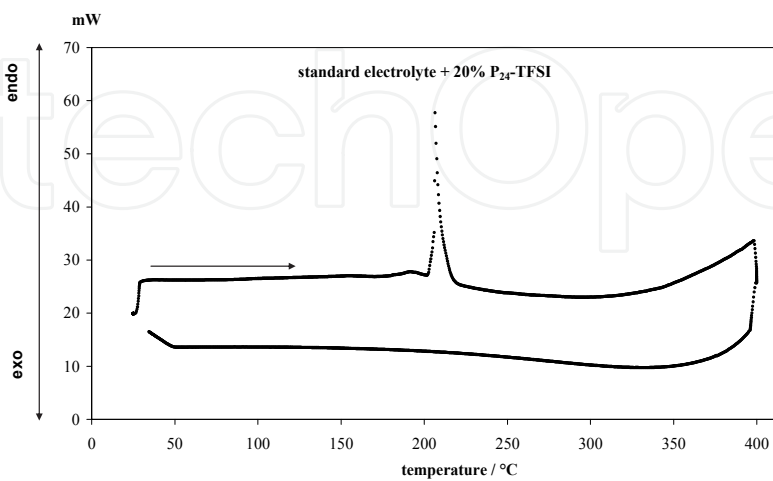
These values show that the most vaporisable solvents are DMC and VC, even if they are already protected by EC and/or PC, they are better prevented from vaporisation in the presence of P_{xy}-TFSI whatever its content, except in the case of the P₁₃-TFSI.



(a)



(b)



(c)

Fig. 1. DSC thermograms of mixtures of standard electrolyte with 20% (w/w) of P_{xy}-TFSI at 5°C/min.

These results clearly show that most of the studies P_{xy} -TFSI, added to the standard electrolyte as co-solvent, can contribute to the improvement of the electrolyte security.

2.2 Tests of flammability

In the event of a thermal incident affecting a Li-ion battery, the first risk is the ignition of the battery. Given the consequences which it can engender, it is essential to evaluate the behaviour of electrolytes in the contact with the flame. For this purpose, in order to investigate the flammability behaviour of P_{xy} -TFSI RTILs, tests are performed with strips of Manila paper soaked with the standard electrolyte containing or not various P_{xy} -TFSI contents from 3.1% to 90% (w/w). All the experimental flammability tests are photographed (or recorded) with a digital camera (Stefan et al., 2009). Some significant photos concerning the resulting tests are presented on Figures 2, 3 and 4. As shown on Figure 2, for the standard electrolyte, the inflammation of the soaked strip of paper is quickstriding (Figure 2a), leading to suffocating white smokes (Figure 2b). Strips soaked by the studied mixtures when the RTIL content is from 3.1% to 10 % present quite the same behaviour in the contact with the flame of the lighter (Figure 3a). Nevertheless, no white smoke is appearing, the electrolyte is gently burning (Figure 3b).

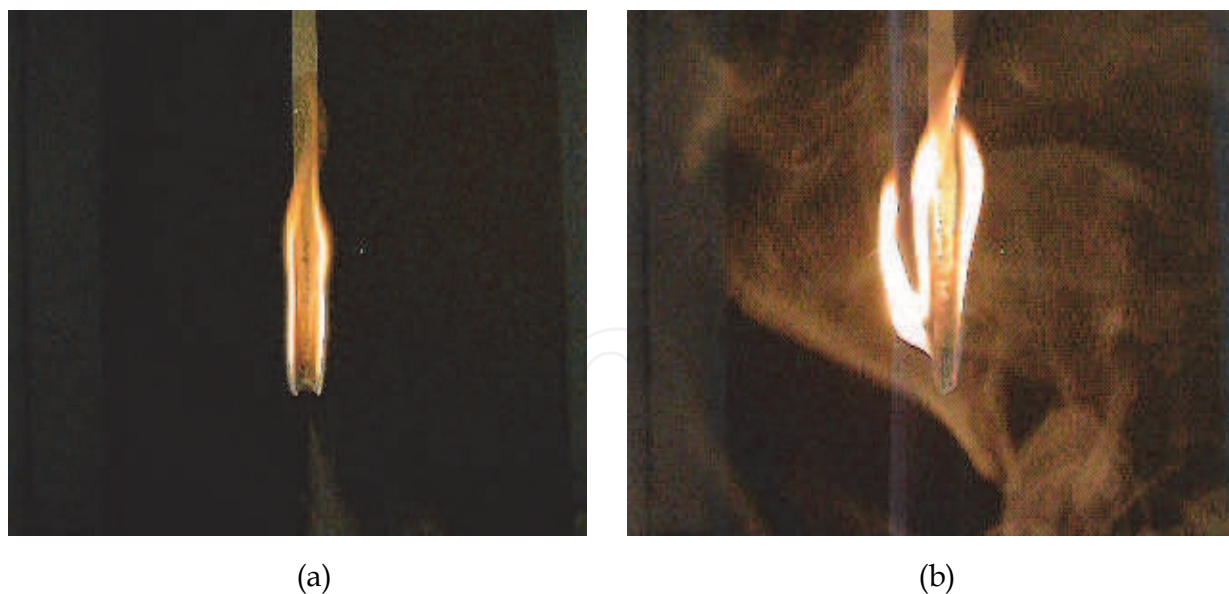


Fig. 2. Test of flammability of the standard electrolyte: (a) lighter flame in contact with the soaked paper, (b) inflammation of the strip.

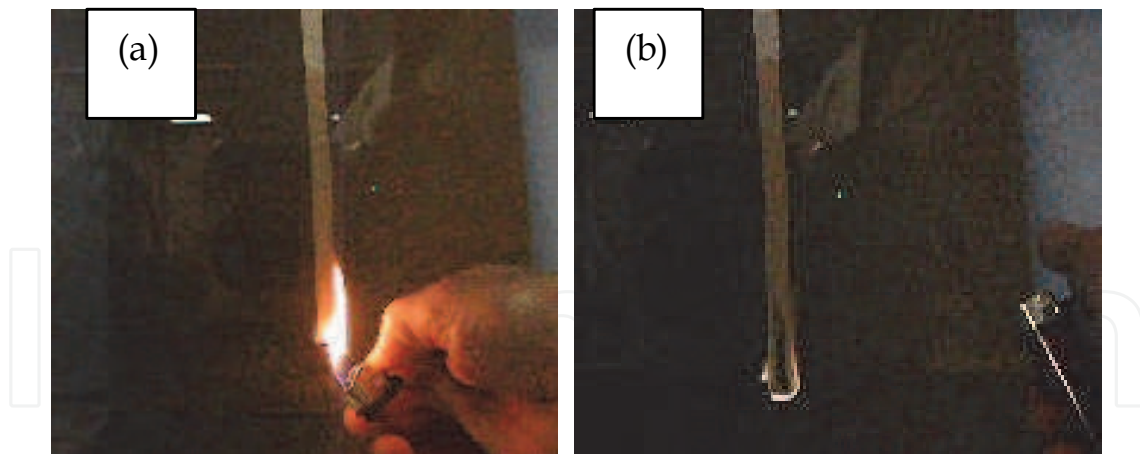


Fig. 3. Test of flammability of mixtures containing 3.1% to 10% of P_{xy} -TFSI: (a): lighter flame in contact with the soaked paper, (b): gentle burn.

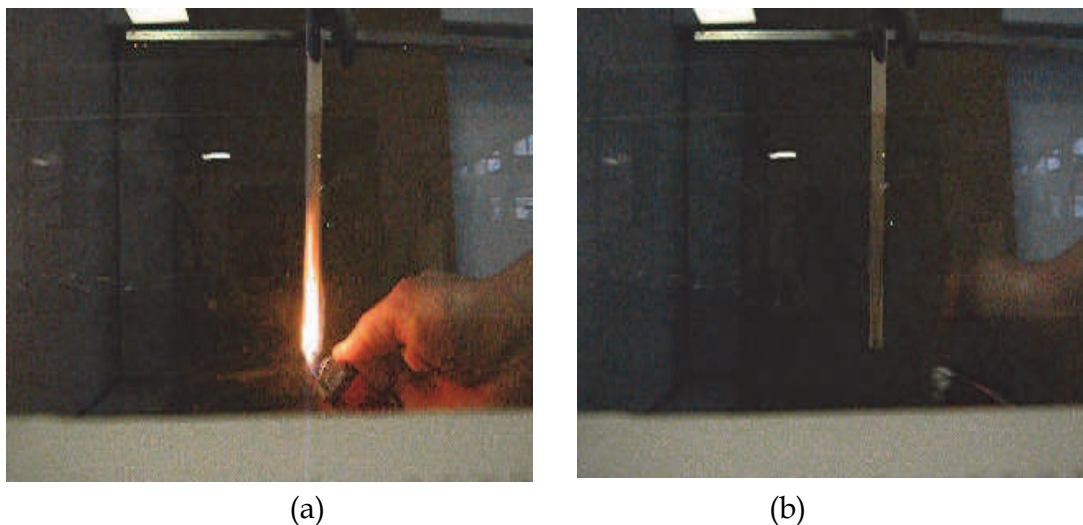


Fig. 4. Test of flammability of mixtures containing 20% to 50% of P_{xy} -TFSI: (a): lighter flame in contact with the soaked paper, (b): flame self-extinguished.

In the case of a RTIL content in the range 20% to 50%, the soaked strips are very difficult to inflame (Figure 4a), then after a very brief inflammation, the tiny flame goes out. For mixtures of P_{xy} -TFSI content over 50 %, the soaked strips of paper present a remarkable resistance to the flame, like the pure P_{xy} -TFSI RTILs do, related to their thermal stability at high temperatures (Stefan et al., 2010). These tests show that under the influence of the heat of the flame of the gas lighter, the most volatile solvent (DMC) is partially vaporized and ignites briefly when the P_{xy} -TFSI RTIL content is over 10% in the mixture.

2.3 Conclusion on the thermal behaviour of mixtures containing P_{xy} -TFSI added as co-solvents in the standard electrolyte

Because of the thermal stability and the very low volatility of the pure P_{xy} -TFSI RTILs, when added as co-solvent to highly flammable organic solvents, such as DMC, PC, EC and VC, the obtained mixtures are more protected from a thermal incident than pure organic molecular solvents. This leads to a very good behaviour of these mixtures in the contact

with the flame of a gas lighter. In particular, the flame extinguishes itself as soon as the content in P_{xy} -TFSI exceeds 20%. Thus P_{13} -TFSI, P_{14} -TFSI, P_{15} -TFSI or P_{24} -TFSI can be flame-retardant for the standard electrolyte, especially for contents over 20%. These very encouraging results for thermal stability purpose have to be confirmed with a study of transport properties of the mixtures under consideration, in order to be incorporated in a Li-ion battery device.

3. The study of the transport properties of electrolytes containing P_{xy} -TFSI added as co-solvents

The conductivity of electrolytes is a fundamental criterion for the electrochemical applications. This conductivity of ionic type is usually strongly correlated to the viscosity of the electrolyte. The two parameters are thus presented afterward in this chapter.

3.1 Study of the ionic conductivity of mixtures

The study of the conductivity of the mixed electrolytes based on standard electrolyte/ P_{xy} -TFSI RTIL is performed as a function of the salt content: either the P_{xy} -TFSI RTIL or $LiPF_6$. The influence of the P_{xy} -TFSI nature on the ionic conductivity is also under consideration. $LiPF_6$, not directly soluble in P_{xy} -TFSI at ambient temperature, the necessary complementary quantity to keep the global content of 1M for the lithium salt, is added at first to the standard electrolyte, and then mixed with the tested P_{xy} -TFSI.

3.1.1 Influence of the P_{14} -TFSI co-solvent content (w/w) on the ionic conductivity

As all the P_{xy} -TFSI RTILs under study can be good flame retardant, P_{14} -TFSI is chosen to investigate the influence of its content (w/w) on the electrolyte ionic conductivity at 20°C only for availability purposes. P_{14} -TFSI content is varying from 0% to 100%. The corresponding conductivity values are presented on the Figure 5.

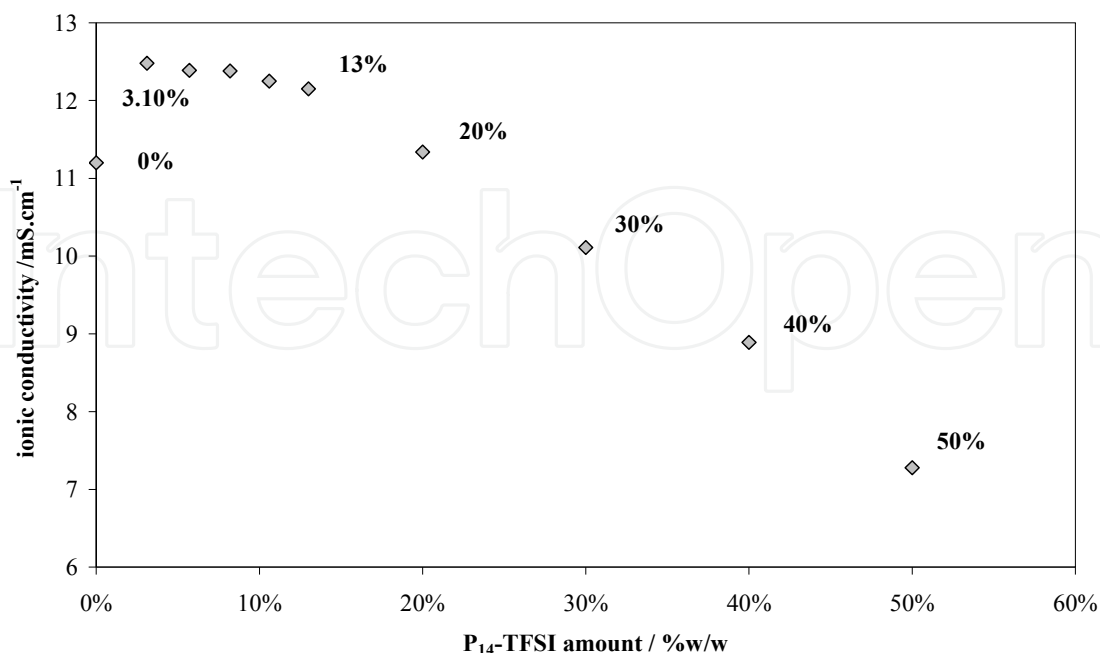


Fig. 5. Ionic conductivity at 20°C of standard electrolyte mixtures with P_{14} -TFSI RTIL of various contents.

On this graph, the conductivity in added co-solvent 0% corresponds to that of the standard electrolyte in 20°C, whereas that at 100% represents the conductivity of pure P₁₄-TFSI at 20°C. As seen on Figure 5, for a content of the co-solvent lower than approximately 20 %, the conductivity of mixtures exceeds that of the standard electrolyte. This range is characterized by the presence of the ionic conductivity maximum, obtained for the lowest content of P₁₄-TFSI, i.e. 3.1%. Then for further addition of P₁₄-TFSI up to 13%, the ionic conductivity decreases slightly leading to a loss of 0.5 mS.cm⁻¹. Between 13% and 20% of P₁₄-TFSI, the conductivity loss increases, it is around 1 mS.cm⁻¹, but the mixture ionic conductivity is still remaining over the standard electrolyte one up to around 30% of P₁₄-TFSI. Over 30%, the decreasing ionic conductivity of mixtures becomes lower than the standard electrolyte one, probably due to a growth of the electrolyte viscosity.

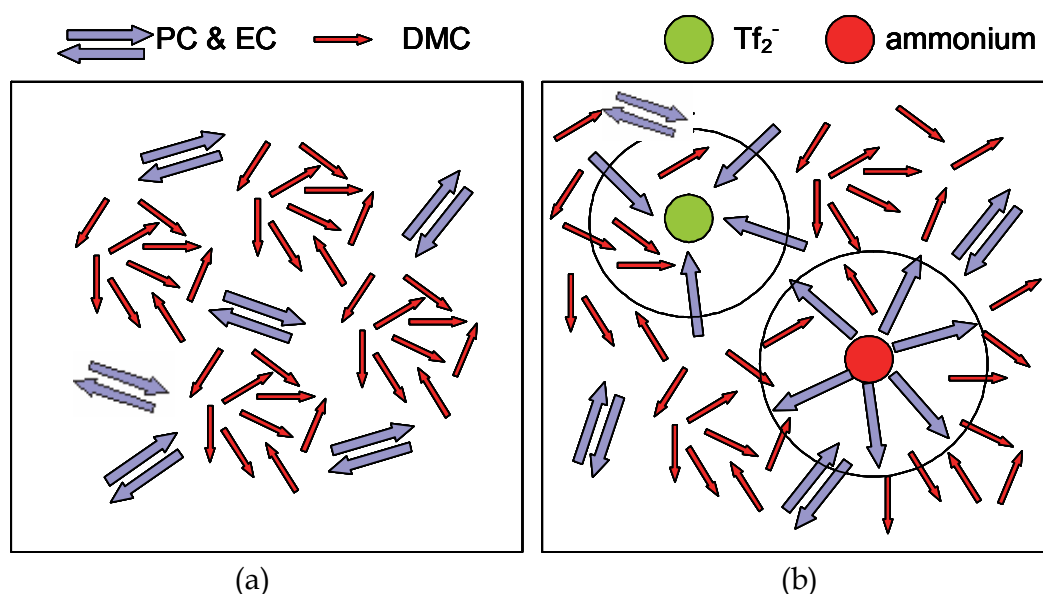
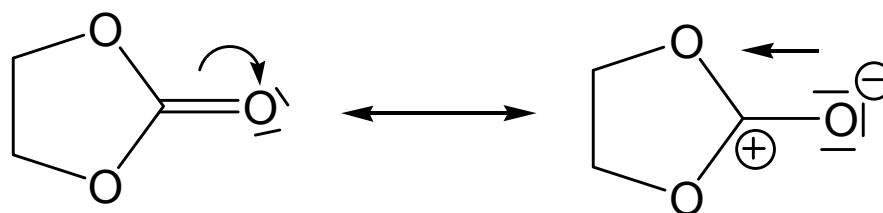


Fig. 6. Schematic arrangement of the solvent molecules, PC, EC, DMC respectively, with regard to the P_{xy}⁺ and TFSI⁻ (i.e. Tf₂⁻) ions: (a) EC/PC/3DMC; (b) EC/PC/3DMC in the presence of P_{xy}⁻TFSI.

To better understand these phenomena, a schematic arrangement related to the structure is presented on the Figure 6. In this schematic layout, blue arrows symbolize the molecules of cyclic alkyl-carbonates, such as PC and EC, whereas the red arrows those of dimethylcarbonate. It is noticeable that PC and EC molecules are turning anti-parallel (Papoular et al., 2005), to favour a more important compactness. Within the framework of the carbonyl group present in the structure of these carbonate-based solvents, the carbon presents sp² hybrid orbital. Besides, the oxygen atom of higher electronegativity than the carbon is going to attract more the π electrons, the C=O bond is thus polarized according to:



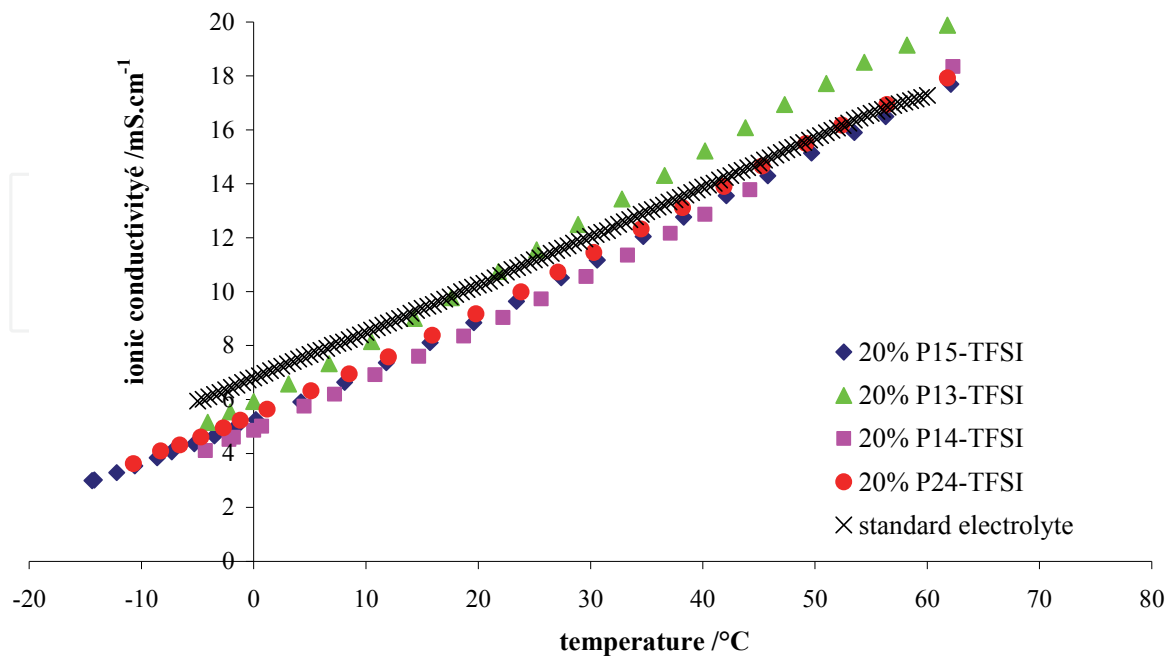
Consequently, the polarization of the carbonyl group is going to infer an electrophilic center on the carbon atom and a nucleophilic center on the oxygen atom. The direction of the blue arrows corresponds to the direction of dipole moments within the PC and EC molecules. This structural property allows several phenomena to be explained, such as the decrease of the mixture density, according to the co-solvent content. Effectively, in the centrosymmetric electric field of the ions, the PC and EC molecules turn, taking up more space in the solution. Therefore, the molar volume of the free solvent is weaker than in the solvation layer, the density is thus decreasing with the addition of the RTIL in the electrolyte. Another consequence due to this phenomenon concerns the strong reduction of the DMC vapour pressure, which involves the decrease of the electrolyte flammability in the presence of P_{xy} -TFSI RTIL. The greater the content of the RTIL, the greater the mixture is flame resistant. Around of the density minimum, they are no more free molecules of solvent, because the ions are entirely solvated. Beyond this minimum, the solvation of the ions is incomplete, and then these charged species can interact by more intense Coulombic strengths, leading to an increase of the viscosity and a decrease of the ionic conductivity because of a drop in the ion mobility.

3.1.2 Influence of the temperature and of the P_{xy} -TFSI co-solvent type on the ionic conductivity

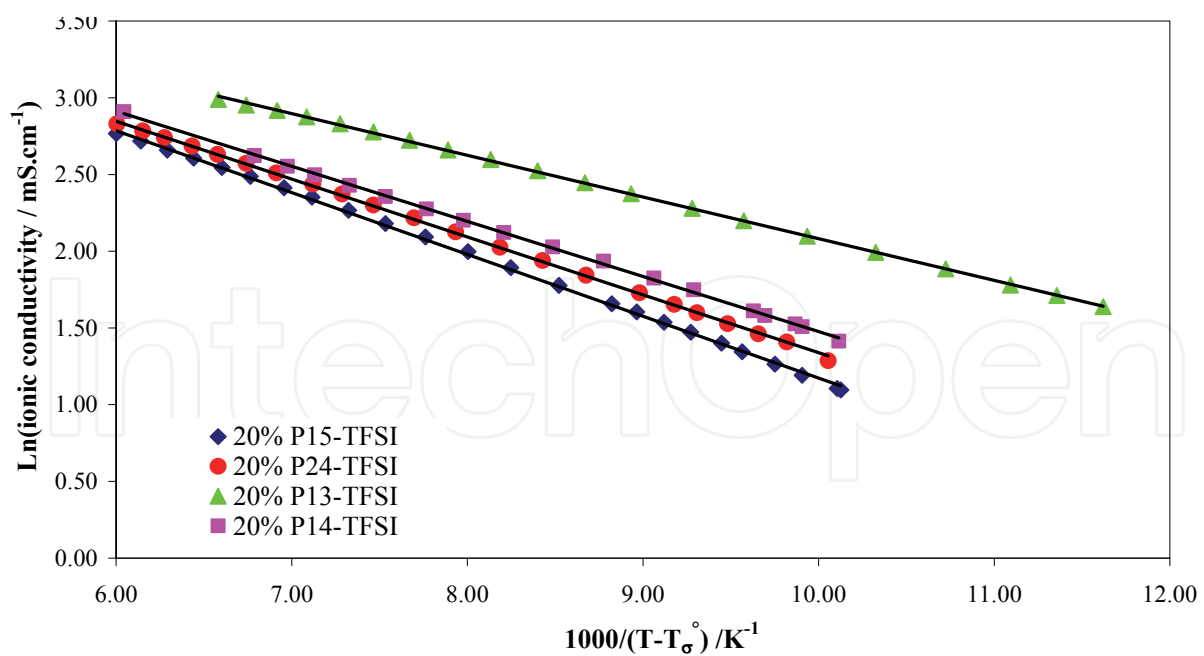
The temperature dependence of the ionic conductivity of mixtures is studied from 10°C to 65°C for various P_{xy} -TFSI RTILs, whose content is firstly fixed at 20% (w/w). The results presented on the Figure 7 show that the conductivity of these mixtures increases with the temperature according to the established order: 20% P_{15} -TFSI < standard electrolyte < 20% P_{24} -TFSI < 20% P_{14} -TFSI < 20% P_{13} -TFSI. This order respects exactly that of the rise of the ionic conductivity obtained for the pure P_{xy} -TFSI RTILs (Mac Farlane et al., 1999; Wu et al. 2003a, 2003b). The experimental results for the ionic conductivity are well fitted by the VTF model as shown on Figure 7. The parameters used here are the temperatures of ideal glassy transition, T_g° , already reported for the conductivity of the pure P_{xy} -TFSI RTILs (Mac Farlane et al., 1999; Wu et al. 2003a, 2003b).

3.1.3 Influence of the lithium salt concentration on the ionic conductivity of the mixtures containing the standard electrolyte and 30 % of P_{14} -TFSI

The influence of the temperature on the mixture ionic conductivity is studied according to the lithium salt concentration from 0.25 M and 1.25 M. For purpose of comparison with the standard electrolyte conductivity (cf. section 3.1.1), the P_{14} -TFSI content is fixed at 30%. The experimental results are depicted in the Figure 8. As expected, from the VTF model, the conductivity increases with the temperature. Furthermore at constant temperature, as the concentration of $LiPF_6$ increases, the conductivity decreases. This effect, often observed in the presence of lithium salts, is essentially attributed to an increase in the viscosity of the media (Taggougui, 2007). The standard electrolyte (Figure 7) presents a lower dependency towards the temperature than the studied mixtures. Over 30°C, mixtures present a higher ionic conductivity than the standard electrolyte, whatever the concentration in added $LiPF_6$ is. On the other hand between 10°C and 30°C, only mixtures of lithium concentration equal or lower than 0.75 M are more conducting than the standard electrolyte. This sensitivity to temperature variations can be quantified by the concept of fragility (Martinez & Angell, 2001; Wu et al. 2003a, 2003b).



(a)



(b)

Fig. 7. Temperature dependence of the ionic conductivity of 20% P_{xy}-TFSI mixtures and of the standard electrolyte; (a) experimental results; (b) fits from the VTF model

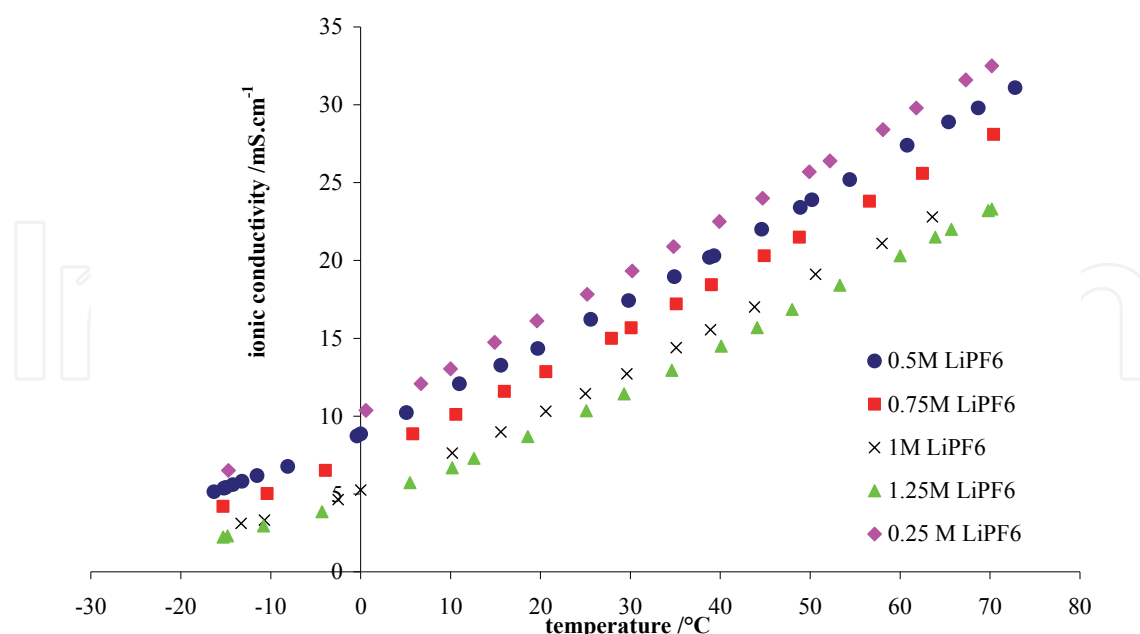


Fig. 8. Temperature dependence of the ionic conductivity of 30% P₁₄-TFSI mixtures as a function of LiPF₆ concentration.

3.2 Study of the dynamic viscosity of mixtures

The high viscosity of the P_{xy}-TFSI RTILS constitutes a real disadvantage for their applications in batteries. The only means to reduce the viscosity are an increase of the temperature or the addition of less viscous solvents. The study of the viscosity of the mixed electrolytes based on the mixture standard electrolyte/P_{xy}-TFSI RTIL is performed as a function of the salt content: either the P_{xy}-TFSI RTIL or LiPF₆. The influence of the P_{xy}-TFSI nature on the viscosity is also under consideration. The Figure 9 summarizes the evolution with the temperature of the viscosity according to the type of P_{xy}-TFSI added at 20%. Even if measures are performed at 2°C/min between 10°C and 90°C (insert in Figure 9), only the results from 10°C to 40°C are significant because of the vaporisation of one of the co-solvents (the DMC essentially, because of its high vapour pressure). Beyond 50°C, the viscosity of mixtures increases in a surprising way. As the used device (TA Instruments) is not equipped for airtight measurements, allowing it to work under an atmosphere saturated in vapour of the most volatile solvents, it is very likely that the observed variations of viscosity are connected to the modifications of the composition of the studied mixtures. Indeed the DMC solvent has already at ambient temperature a high vapour pressure (18 mmHg in 21.1°C (Weast, 1976)). As a result after 40°C the electrolyte becomes impoverished in DMC, the solvent of lower viscosity, so that the dynamic viscosity of the mixtures increases beyond 50°C. Globally, electrolytes containing more RTILs are more viscous also. To bring to light the effect of the concentration of the lithium salt, LiPF₆, on the dynamic viscosity of mixtures containing 30% P₁₅-TFSI increasing amounts of LiPF₆ are added to mixtures from 0.25 M to 1.25 M. The corresponding results are reported in Figure 10 where they are compared to the dynamic viscosity of the standard electrolyte. For a 20% content, the viscosity decreases according to the order: P₁₃-TFSI > P₂₄-TFSI > standard electrolyte > P₁₅-TFSI > P₁₄-TFSI. As expected for the same amount of LiPF₆, the dynamic viscosity increases with the weight content of P_{xy}-TFSI.

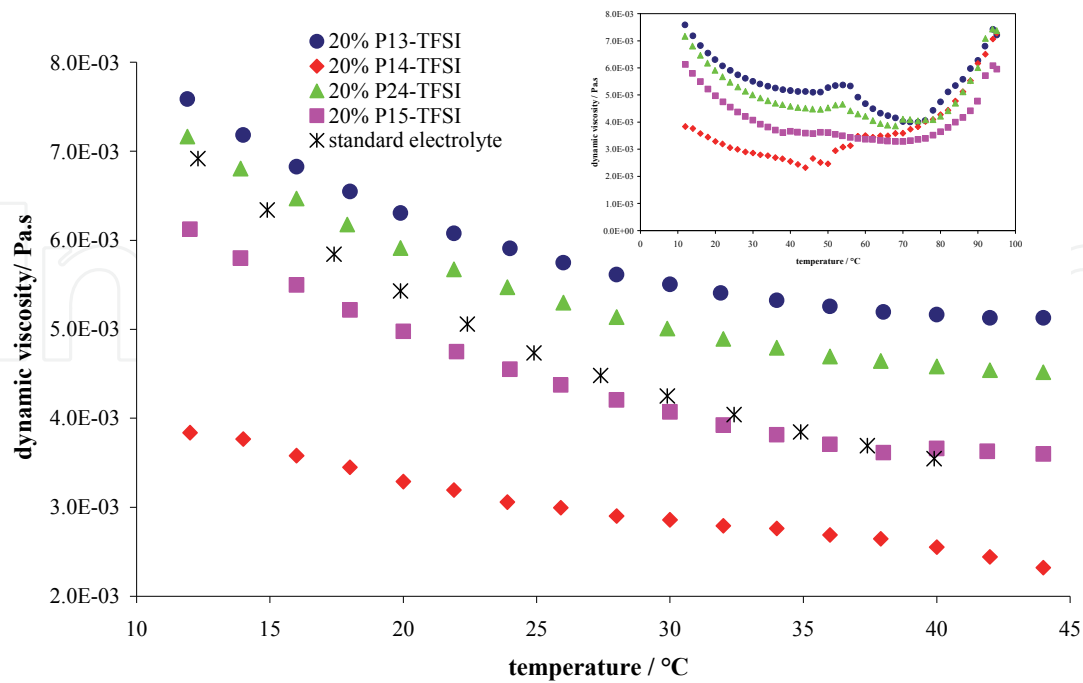


Fig. 9. Temperature dependence of the dynamic viscosity of 20% P_{xy} -TFSI mixtures, at $2^{\circ}\text{C}/\text{min}$ (insert: full temperature range).

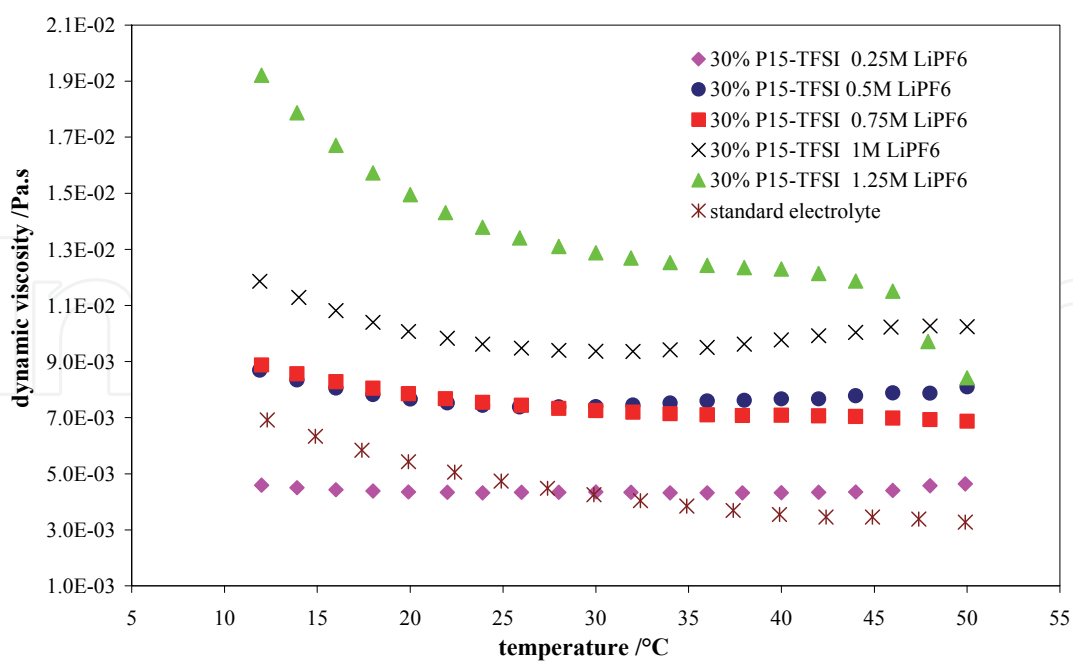


Fig. 10. Temperature dependence of the dynamic viscosity of 30% P_{15} -TFSI mixtures as a function of LiPF_6 concentration.

Globally these results confirm the fact that the viscosity increases with the lithium salt concentration. The addition of lithium salt in the electrolyte leads to a progressive increase of the mixture viscosity, which results in a decrease of the conductivity as mentioned previously (cf. section 3.1.3).

3.3 Conclusion on the transport properties of mixtures containing P_{xy}-TFSI added as co-solvents in the standard electrolyte

The weak ionic conductivity of the pure P_{xy}-TFSI RTILs can be improved if these RTILs are mixed with molecular solvents (or mixtures of molecular solvents). Mixtures containing up to 30% P_{xy}-TFSI present conductivity superior or equal to that of the standard electrolyte. The viscosity of the standard electrolyte does not vary in a significant way when P_{xy}-TFSI RTIL is added as co-solvent, for a content limited to 20% or 30% (w/w). All these results show that the moderate addition of P_{xy}-TFSI RTILs does not decrease the performances obtained in ionic conduction for the industrial standard electrolyte EC/PC/3DMC + LiPF₆ 1M + 1% VC. So, it is definite that the ionic transport in the studied mixtures does not constitute an obstacle to the use of co-solvent based on P_{xy}-TFSI RTILs for Li-ion batteries applications. But before their use in electrochemical devices, their compatibility with electrode and separator materials must be checked specifically for wettability purposes.

In order to better understand the effect of small cations, such as Li⁺, and of molecular solvent addition on the conductivity and the dynamic viscosity of P_{xy}-TFSI, PGSE-NMR measurements are performed. The self-diffusion coefficients of lithium ⁷Li (D(Li)) and hydrogen ¹H (D(H)) nuclei, are determined by PGSE-NMR. D(Li) is related to the diffusion of the Li⁺ cation and D(H) is related to the diffusion of pyrrolidinium cation of the considered RTIL. P₁₅-TFSI is chosen as model IL for these experiments. In Figure 11(a), the variations of the self diffusion coefficient for ¹H and ⁷Li are reported as a function of the concentration of LiTFSI in P₁₅-TFSI. Both self diffusion coefficient decrease linearly when the concentration in LiTFSI is increased. This is expected from the Stokes Einstein relation if the dynamic viscosity follows itself a linear dependence on the salt concentration as predicted by the semi-empirical relation (Jones & Dole, 1929; Kaminski, 1957): $\eta_r = \eta/\eta^0 = 1 + A C^{1/2} + BC$. If the term in $C^{1/2}$ is negligible, η^0 is the viscosity of the pure RTIL, C the concentration in lithium salt, A can be calculated (Falkenhagen & Vernon, 1932) and B can be considered as an adjustable parameter linked to the molar volume of the added salt. It is noticeable that the RTIL self diffusion coefficient follow the same trend and hence verifies also the Stokes-Einstein relation. Nevertheless the slopes of the two lines are different and this means that the increase in viscosity has a different impact on the two diffusion coefficients, the Li salt being less affected than the RTIL. In order to test the influence of the anion of the Li salt, LiPF₆ is added to P₁₅-TFSI instead of LiTFSI. Results are presented as graphs in Figure 11(b). The self diffusion coefficient of the RTIL follows a linear variation with a slightly smaller slope but this is not the case of the Li⁺ self diffusion coefficient which is quite constant between 0.25 M and 0.50 M, and then decreases.

As illustrated in Figure 12, the variation of the D(Li)/D(H) ratios is quite different for LiTFSI and LiPF₆ in the presence of P₁₅-TFSI: it increases with LiPF₆ and decreases with LiTFSI. This implies that Li⁺ environment is changing when PF₆⁻ is added to the RTIL. D(Li) is thus raising more than D(H), which reflects the self-diffusion coefficient of P₁₅⁺. According to the HSAB theory, TFSI⁻ is a softer base than PF₆⁻, because its negative charge is delocalized all

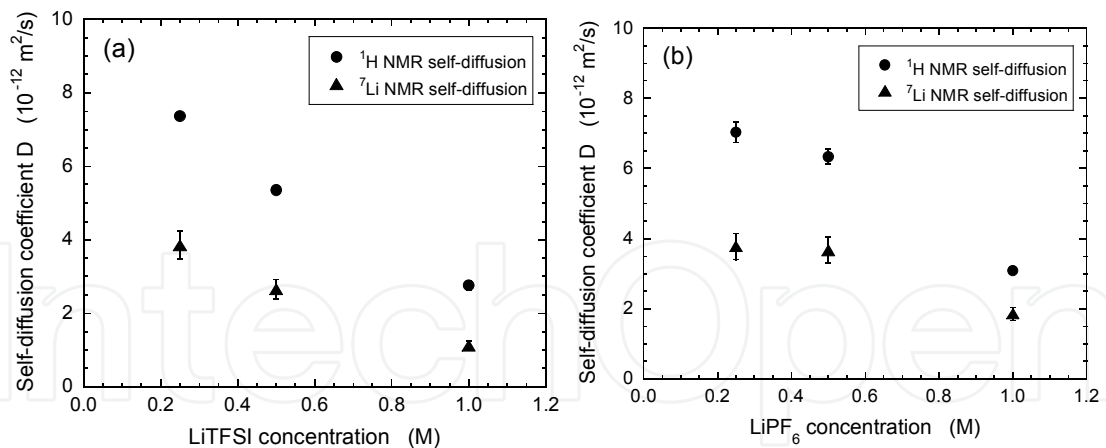


Fig. 11. Evolution of the self-diffusion coefficients at 25°C for the solvent molecules (^1H NMR) and the lithium cations (^7Li NMR) in the LiTFSI/ P_{15} -TFSI mixture samples as a function of the LiTFSI concentration (a), and in the LiPF₆/ P_{15} -TFSI mixture samples as a function of the LiPF₆ concentration (b).

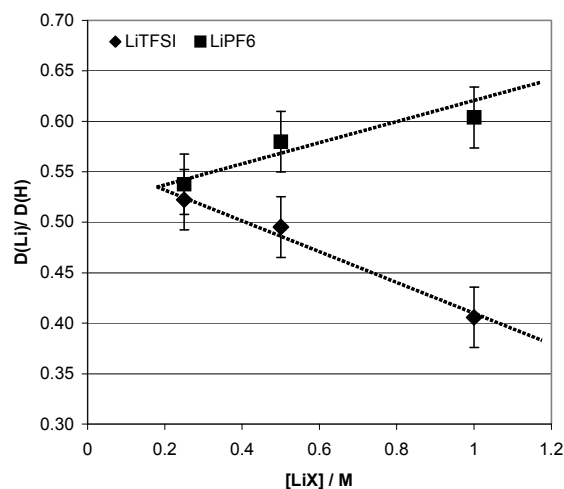


Fig. 12. Evolution of the ratio of lithium and hydrogen self-diffusion coefficients as a function of either the nature or the amount of the added salt to P_{15} -TFSI at 25°C .

over the anion structure, it is thus expected that preferential interactions occur between the hard acid (Li^+) and the hard base (PF_6^-) than the softer TFSI⁻ base. Thus when LiPF₆ is added, the probability to get a tight $\text{Li}^+\text{-PF}_6^-$ ion pair becomes more important, and especially over $C=0.50 \text{ M}$ in lithium salt. Because of its overall zero charge, the ion pair does not interact by Coulombic forces with the RTIL ions and this leads to an increase in the $D(\text{Li})/D(\text{H})$ ratio. At the opposite, when LiTFSI is added, the Li^+ ion is intercalating within the free spaces of the RTIL ionic structure leading to the re-enforcement of the columbic interactions and to a decrease in $D(\text{Li})/D(\text{H})$. In order to check the dynamic viscosity effect on $D(\text{Li})$ and $D(\text{H})$, P_{15} -TFSI is replaced by an alkylcarbonate solvent ternary mixture: EC/PC/3DMC (by weight). The corresponding results, reported in Table 4, show that, when the RTIL is replaced by the fluid alkyl carbonate mixture, the self-diffusion coefficients of both lithium and hydrogen atoms increase within a ratio of 100. Molecular solvents are preferentially

solvating Li^+ and the Coulombic interaction with the RTIL ions are reduced leading to an enhanced mobility.

	$\text{P}_{15}\text{-TFSI} + 1 \text{ M LiPF}_6$	$\text{EC/PC/3DMC} + 1 \text{ M LiPF}_6$
from ^7Li NMR	$1.9 \cdot 10^{-12}$	$1.9 \cdot 10^{-10}$
from ^1H NMR	$3.1 \cdot 10^{-12}$	$4.9 \cdot 10^{-10}$

Table 4. Self-diffusion coefficients, in $\text{m}^2 \cdot \text{s}^{-1}$, for molecular solvents and P_{15}^+ cation (from ^1H NMR), as well as for the lithium cation (from ^7Li NMR), in the presence of 1 M LiPF_6 .

4. Wettability of separators and electrodes by mixtures

The role of the separator is to electrically isolate the anode from the cathode while allowing the charged species to go through. The separator must be perfectly wet by the electrolyte to avoid any slowing down of the ionic transport. Characterization and prediction of wetting phenomenon by contact angle (CA) measurements, according to the sessile drop method using a G-11 goniometer (Krüss, Germany), and surface free energy (γ_L) calculations, from measurement with a tensiometer K10ST (Krüss, Germany) with the ring method, are powerful analysis tools widely used for many applications (Good, 1992). Thus, to comprehend the wettability of separators and electrodes commonly used in Li-Ion battery devices, it is also necessary to study the surface free energy of the $\text{P}_{xy}\text{-TFSI}$ RTILs and to characterise the smooth polymeric materials as described elsewhere (Stefan et al., 2009).

4.1 Free surface energy of the mixtures

The values of free surface energy obtained at 25°C for mixtures based on 20 % $\text{P}_{xy}\text{-TFSI}$ RTIL and for the standard electrolyte are reported in Table 5.

$\gamma_L / \text{mN} \cdot \text{m}^{-1}$	$\text{P}_{13}\text{-TFSI}$	$\text{P}_{14}\text{-TFSI}$	$\text{P}_{15}\text{-TFSI}$	$\text{P}_{24}\text{-TFSI}$	std.electrolyte.
pure $\text{P}_{xy}\text{-TFSI}^*$	36.5 ± 0.1	34.5 ± 0.1	34.6 ± 0.1	35.2 ± 0.1	36.9 ± 0.1
20% $\text{P}_{xy}\text{-TFSI}$	37.7 ± 0.1	37.7 ± 0.2	28.4 ± 0.1	38.0 ± 0.1	(-)

Table 5. Surface free energy of the pure or mixed P_{xy} RTILs and of standard electrolyte (in $\text{mJ} \cdot \text{m}^{-2}$) at 25°C ; * from (Stefan et al., 2009).

Except the mixture containing the $\text{P}_{15}\text{-TFSI}$, the free surface energy of mixtures is close to that of the standard electrolyte and those of the pure $\text{P}_{xy}\text{-TFSI}$ RTILs. This indicates that the surface layer probably consists mainly of the ionic liquid. The mixture based on 20% $\text{P}_{15}\text{-TFSI}$ presents a free surface energy sharply lower than the others in connection with the longest substituted carbon chain, it should thus better wet the separator.

4.2 Contact angle of mixtures on solid supports

The tests are done on smooth polymeric materials, i.e. polyethylene (PE) and polypropylene (PP) at -4°C . This choice of temperature is due to the fact that problems of non wettability generally occur at low temperatures. In Table 6 are reported the results contact angles (in degree) at the liquid/polymer/air interface, in the case of the standard electrolyte and the mixtures of various $\text{P}_{14}\text{-TFSI}$ and $\text{P}_{24}\text{-TFSI}$ contents. The CA values of liquids on PE are from

4 ° to 11 ° lower than those obtained on PP. PE is thus better wet than PP because of a higher free surface energy (for EP: 33 mJ.m⁻², for PP: 30 mJ.m⁻² (Cognard, 2000).

CA/ ° (±1)	Std. electrolyte	8%		21%		30%	
		P ₁₄ -TFSI	P ₂₄ -TFSI	P ₁₄ -TFSI	P ₂₄ -TFSI	P ₁₄ -TFSI	P ₂₄ -TFSI
PE	38.3	41.1	41.5	42.3	48.3	42.7	47.6
PP	49.3	50.1	50.6	51.4	52.1	49.6	53.6

Table 6. Contact angles (in degree) at the liquid/polymer/air interface, for the standard electrolyte and the mixtures of various P₁₄-TFSI and P₂₄-TFSI contents, at -4°C.

The standard electrolyte presents the lower CA, whether it is on EP or on PP. But these differences between CA remain less 10°, the standard electrolyte wetting better the polyolefins than the mixtures containing P_{xy}-TFSI RTILs. The amount of P_{xy}-TFSI RTIL in the mixture does not affect the CA values; however the mixtures based on the P₂₄-TFSI RTIL present the highest values of CA, whether it is on EP or PP. In all cases, the results of Table 6 show that the CA on smooth polymeric materials are large enough up (>20-30°), that wetting problems could be engendered when the temperature is low on a porous support as the separators.

4.3 Wettability of Celgard® separators at 25°C

To estimate at the wettability of separators commonly used in Li-ion batteries, the contact angles are measured at 25°C on porous supports (i.e. Celgard® separator whose characteristics are reported in (Stefan et al., 2009) at the liquid/polymer/air interface, where the liquid is either the standard electrolyte, the ternary EC/PC/3DMC solvent or the pure P_{xy}-TFSI RTILs. The analysis of the results presented in Table 7 shows that the Celgard®2730 separator is the best wet, which seems evident because PE is the smooth polymeric material the best wet (Table 6). The addition of a salt (i.e. LiPF₆ or P_{xy}-TFSI) increases the CA values. The best wetting liquids are the ternary mixture EC/PC/3DMC and the P₁₅-TFSI RTIL, which already presents the relatively low free surface energy (Table 5). So, Celgard®2730/P₁₅-TFSI seems to be the best set for wettability purposes. The other P_{xy}-TFSI/Celgard® sets can not be ignored because the corresponding CA values are not too far from those obtained with the standard electrolyte. To study the influence of P_{xy}-TFSI RTIL content on the separator wettability, two mixtures based on of P₁₄-TFSI are chosen (i.e. 15% and 21%). The experimental results, obtained at 25°C, are gathered on Table 8.

CA/ °	Celgard®2730 PE 43% porosity	Celgard® 2320 PP-PE-PP 41% porosity	Celgard®2500 PP 55% porosity	Celgard® 2400 PP 37% porosity
	Std. electrolyte	43.6 ± 1.0	50.6 ± 2.0	53.5 ± 0.9
EC/PC/3DMC	42.0 ± 1.1	46.0 ± 1.5	45.6 ± 0.9	47.5 ± 0.8
P ₁₃ -TFSI	53.1 ± 0.7	60.9 ± 1.1	67.3 ± 0.8	60.9 ± 1.0
P ₁₄ -TFSI	46.9 ± 1.7	60.5 ± 0.7	58.5 ± 2.3	59.0 ± 1.3
P ₁₅ -TFSI	38.4 ± 1.4	49.0 ± 0.4	50.5 ± 1.4	52.6 ± 0.6
P ₂₄ -TFSI	46.4 ± 1.1	52.3 ± 0.7	53.9 ± 0.6	56.9 ± 1.0

Table 7. Contact angles (in degree) at the liquid/ Celgard® separators/air interface, for the standard electrolyte, the ternary molecular solvent mixture and the pure P_{xy}-TFSI RTILs, at 25°C.

Results from Table 8 show that the CA decreases when the amount of P₁₄-TFSI RTIL increases from 15% to 21%. In the case of the Celgard®2320 and Celgard®2400, CA for 21% of P₁₄-TFSI is lower than that measured for 100% of P₁₄-TFSI, but it is the opposite for the Celgard®2500 and Celgard®2730. All the presented results are not too far from those obtained with the standard electrolyte. Nevertheless, the weakest values of CA are obtained with the Celgard®2730, PE based, and with the Celgard®2320, a trilayered separator. Furthermore, the effect of the porosity (i.e. Celgard®2500 and Celgard®2400, both PP based) is not significant enough to be further considered.

CA / ° (±1)	Celgard®2320	Celgard®2400	Celgard®2500	Celgard®2730
15% P ₁₄ -TFSI	53.3	62.4	63.3	52.9
21% P ₁₄ -TFSI	49.3	57.6	59.0	48.3
100% P ₁₄ -TFSI	60.5	59.0	58.5	46.9

Table 8. Contact angles (in degree) at the liquid/ Celgard® separators/air interface dependence on the P₁₄-TFSI RTIL content, at 25°C.

4.4 Wettability of the membrane Separion® at 25°C

The wettability of the Celgard® separators based on PE or PP being insufficient for a practical use, especially at low temperatures in the presence of mixtures containing P_{xy}-TFSI, it looks interesting to investigate in a new generation of separator, i.e. the Separion® separator made of porous alumina/silica ceramic coated by a polyethylenterephtalat (PET) polymer. For all the studied liquids (pure or mixed P_{xy}-TFSI RTILs, the ternary solvent mixture EC/PC/3DMC and the standard electrolyte), the contact angles are very difficult to measure on the Separion® separator as already mentioned (Stefan et al., 2009). All the initial CA values are systematically weaker than those observed for separators Celgard®. Thus, in the case of the ternary solvent EC/PC/3DMC and the standard electrolyte, the wetting is immediate leading to an initial contact angle value of 0°. In the case of the 20% and 30% P_{xy}-TFSI RTIL mixtures, the initial contact angle values are always lower than 10°.

4.5 Wettability of the positive and negative electrodes for Li-ion batteries at 25°C

The wettability is a key factor for improving the cycling ability and the power of Li-ion batteries. The wetting of electrodes commonly used for Li-ion battery devices is studied as a function of the P_{xy}-TFSI RTIL content. The experimental results are gathered in Table 9 and Table 10, where the CA values for pure P_{xy}-TFSI RTILs are mentioned for comparison purposes (Stefan et al., 2009).

CA/ ° (±1)	P ₁₃ -TFSI	P ₁₄ -TFSI	P ₁₅ -TFSI	P ₂₄ -TFSI
100% P _{xy} -TFSI	18.3	17.1	15.1	14.7
20% P _{xy} -TFSI	Total wetting			
30% P _{xy} -TFS	Good wetting: initial contact angle values are around 7°.			

Table 9. Contact angles (in degree) at the liquid/ LiCoO₂ electrode/air interface dependence on the P_{xy}-TFSI RTIL content and nature, at 25°C.

As seen in Table 9, the wettability of the composite positive electrode does not raise the problem; the penetration of liquids in the porosity of the electrode is very fast whatever the P_{xy} -TFSI RTIL used and its amount. Because oxides such as $LiCoO_2$ is a ceramic presenting a very high interfacial free energy, that facilitates the wetting (Stefan et al., 2009). For the graphite wetting, the angles of contact obtained with mixtures based on 20% and 30% P_{xy} -TFSI are lower than CA with the pure corresponding P_{xy} -TFSI RTIL, and, slightly superior to the CA obtained with the standard electrolyte (i.e. 10.5°). In every case, the wetting is good enough to let us suppose that the use of mixtures based on P_{xy} -TFSI RTIL should not raise problem of wetting even low-temperature.

4.6 Conclusion on wettability measurements

Results of the wettability of both the negative and the positive electrodes commonly used in Li-ion batteries allows the use of the electrolyte mixtures based on 20% or 30% of P_{xy} -TFSI RTILs. However all the Celgard[®] separators are insufficiently wet by these mixed electrolytes. This problem can be easily resolved by the replacement of this type of polyolefin separator by a ceramic-type separator, such as the Separion[®]. All these promising results let us trust the good electrochemical performances with the use of P_{xy} -TFSI/standard electrolyte mixtures.

CA/ ° (± 1)	P_{13} -TFSI	P_{14} -TFSI	P_{15} -TFSI	P_{24} -TFSI
100% P_{xy} -TFSI	21.1	20.6	17.9	20.2
20% P_{xy} -TFSI	15.0	13.5	11.0	15.1
30% P_{xy} -TFSI	16.0	14.4	11.3	15.5

Table 10. Contact angles (in degree) at the liquid/graphite electrode/air interface dependence on the P_{xy} -TFSI RTIL content and nature, at $25^\circ C$.

5. Electrochemical studies on mixtures

To validate the P_{xy} -TFSI- RTIL mixtures as electrolytes for batteries Li-ion application, tests of cycling ability are required, after the determination of their electrochemical window. The quality of the passivating protective layer, and its stability at the graphite electrode, must be checked by mean of galvanostatic chronopotentiometric measurements. The P_{xy} -TFSI- RTIL contents lower than 20 % (w/w) are not of a real interest, in spite of an ionic conductivity over the standard electrolyte one, because the phenomenon of self-extinguished flame becomes striking only from 20 % of P_{xy} -TFSI. For between 20 % and 30 % P_{xy} -TFSI- RTIL, the performances are optimized from the point of view of the ionic transport, of the thermal stability and of the material wettability Beyond these contents, up to 50 %, the increase of the viscosity of mixtures can limit their applications at room temperature (mainly because of the decrease of the performances of ionic transport), but their use can be considered for higher temperature applications.

5.1 Electrochemical windows of the P_{xy} -TFSI RTILs

RTIL electrochemical windows are obtained from linear sweep voltamperometry performed under argon atmosphere. The rotating working disk electrode (1000 rpm) is made of glassy carbon. A Pt electrode is used as a counter electrode. An Ag/AgCl electrode, in the presence

of saturated KCl in the RTIL, is used as a reference electrode (AgCl and KCl are sparingly soluble in these media). This electrode, especially designed for non-aqueous RTILs, is composed of salt-bridged compartments filled up with P₁₄-TFSI. The smallest one contains the silver wire and AgCl and KCl crystals are added up to saturation. This reference electrode is calibrated against the standard hydrogen electrode (SHE) using the ferrocene redox system (Fc/Fc⁺). The Fc/Fc⁺ (Snook et al., 2006) standard redox potential is taken as E°(Fc/Fc⁺) = 0.45V vs. SHE whatever the solvent used. From Figure 13, the standard potential of Fc/Fc⁺ system is 330 mV vs. the Ag/AgCl(P₁₄-TFSI), KCl(P₁₄-TFSI), reference electrode, leading to a potential of 120 mV vs. SHE or 3.14 V vs. Li/Li⁺ which agrees well with 3.1 V elsewhere determined (Appetecchi et al., 2006).

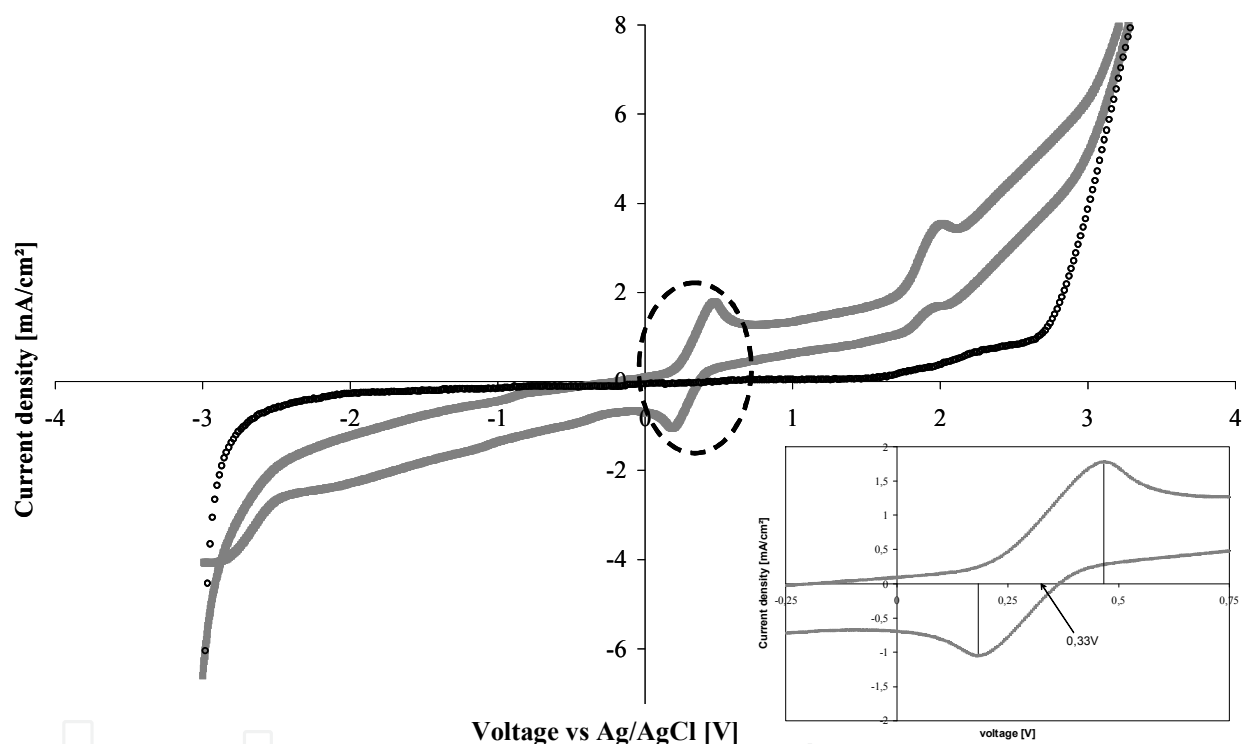


Fig. 13. Cyclic sweep voltammogram at 22°C of pure P₁₄-TFSI and P₁₄-TFSI + ferrocene; W.E.: glassy carbon; C.E.: Pt; R.E.: Ag/AgCl(P₁₄-TFSI), KCl(P₁₄-TFSI); at 100 mV.s⁻¹ and 1000 rpm.

The electrochemical windows of the P_{xy}-TFSI RTILs, at the glassy carbon electrode, are displayed in Figure 14. The anodic limit is nearly the same for all P_{xy}-TFSI electrolytes. This suggests that it is the TFSI⁻ ion which is first oxidized at 2.7 V vs. Ag/AgCl(P₁₄-TFSI)(KCl sat.) electrode (i.e. 5.84 V vs. Li/Li⁺). The cathodic limit is nearly the same at -3 V (0.14 V vs. Li/Li⁺) for P₁₄⁺, P₁₅⁺ and P₂₄⁺, but clearly different for P₁₃⁺ as in this case the reduction of the IL occurs at -2.4 V (0.74 V vs. Li/Li⁺). This shows that the P₁₃-TFSI is less stable toward reduction at the glassy carbon electrode than the other RTILs. This compound will easily react to form a solid electrolyte interface (SEI) which is a passivating protective layer on metallic lithium or at a graphite electrode when the potential is driven to the intercalation potential of lithium ions in graphite.

5.2 Cycling ability study of graphite or LiCoO₂ electrodes in the presence of the mixtures

Button-type half cells composed of a metallic lithium anode and graphite or LiCoO₂ cathodes are used to test the behaviour of elaborated mixtures. The lithium metallic electrode plays the role of the reference electrode.

To ensure the formation of the passivating protective layer (SEI) on the graphite electrode, the first charge/discharge cycle is performed at 60°C, then after the following cycles at 25°C. For transport property and thermal behaviour purposes, the tested electrolytes are mixtures of 20% to 30% P_{xy}-TFSI RTILs, while the charge and discharge processes of the half cells are operated at the same rate C/20, D/20. Figure 15 and Figure 16 illustrate the resulting galvanostatic chronopotentiograms obtained respectively with the LiCoO₂ positive electrode and the graphite negative electrode at 25°C.

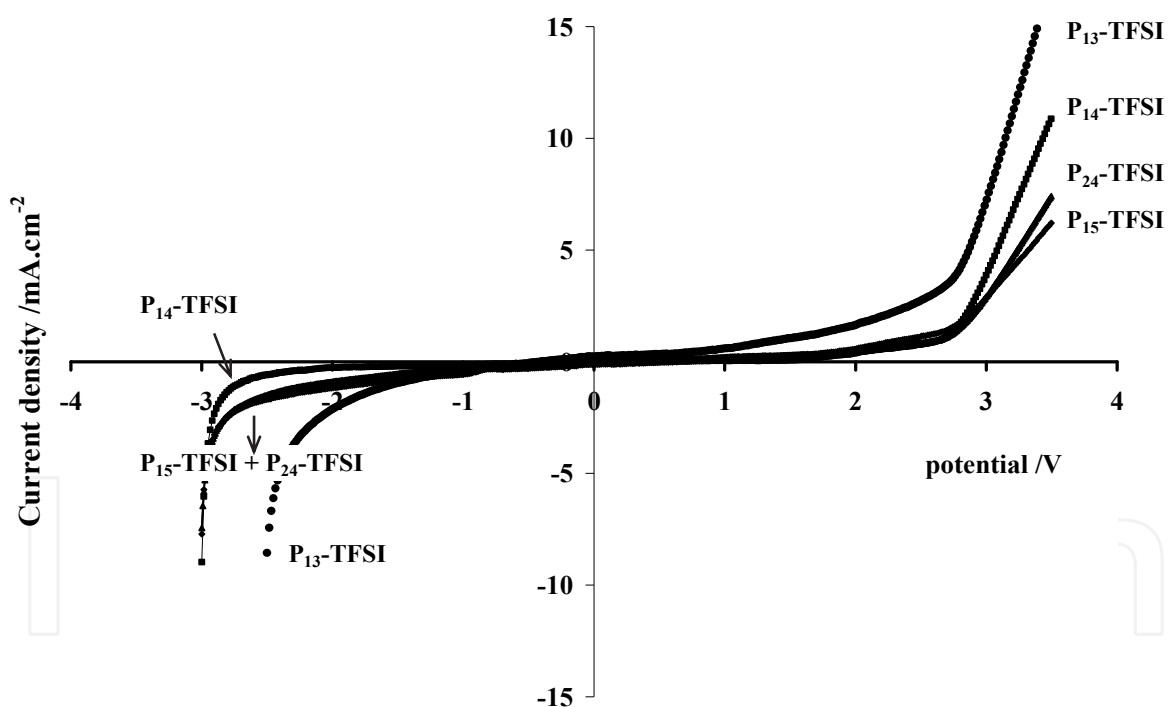


Fig. 14. Linear sweep voltammogram at 22°C of a several P_{xy}-TFSI RTILs tested in this study; W.E., glassy carbon; C.E., Pt; R.E., Ag/AgCl(P₁₄-TFSI), KCl_(sat. in P₁₄-TFSI); scan rate, 100 mV.s⁻¹; at 1000 rpm.

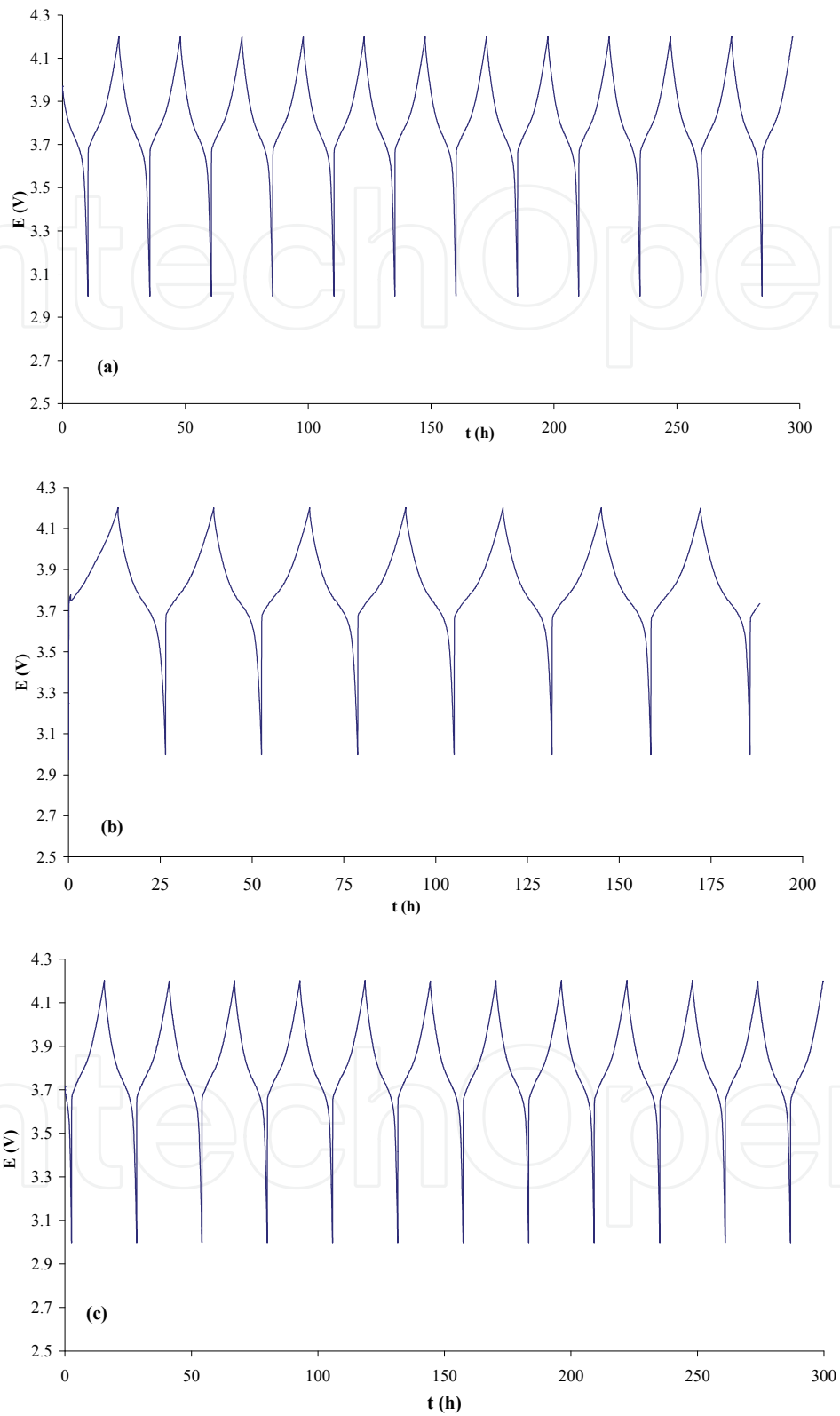


Fig. 15. Galvanostatic chronopotentiometry of a LiCoO_2 electrode, at C/20 and D/20 rates, at 25°C , with an electrolytic solution containing (a) 20% $\text{P}_{14}\text{-TFSI}$; (b) 30% $\text{P}_{14}\text{-TFSI}$; (c) 40% $\text{P}_{14}\text{-TFSI}$; reference electrode: Li/Li^+ .

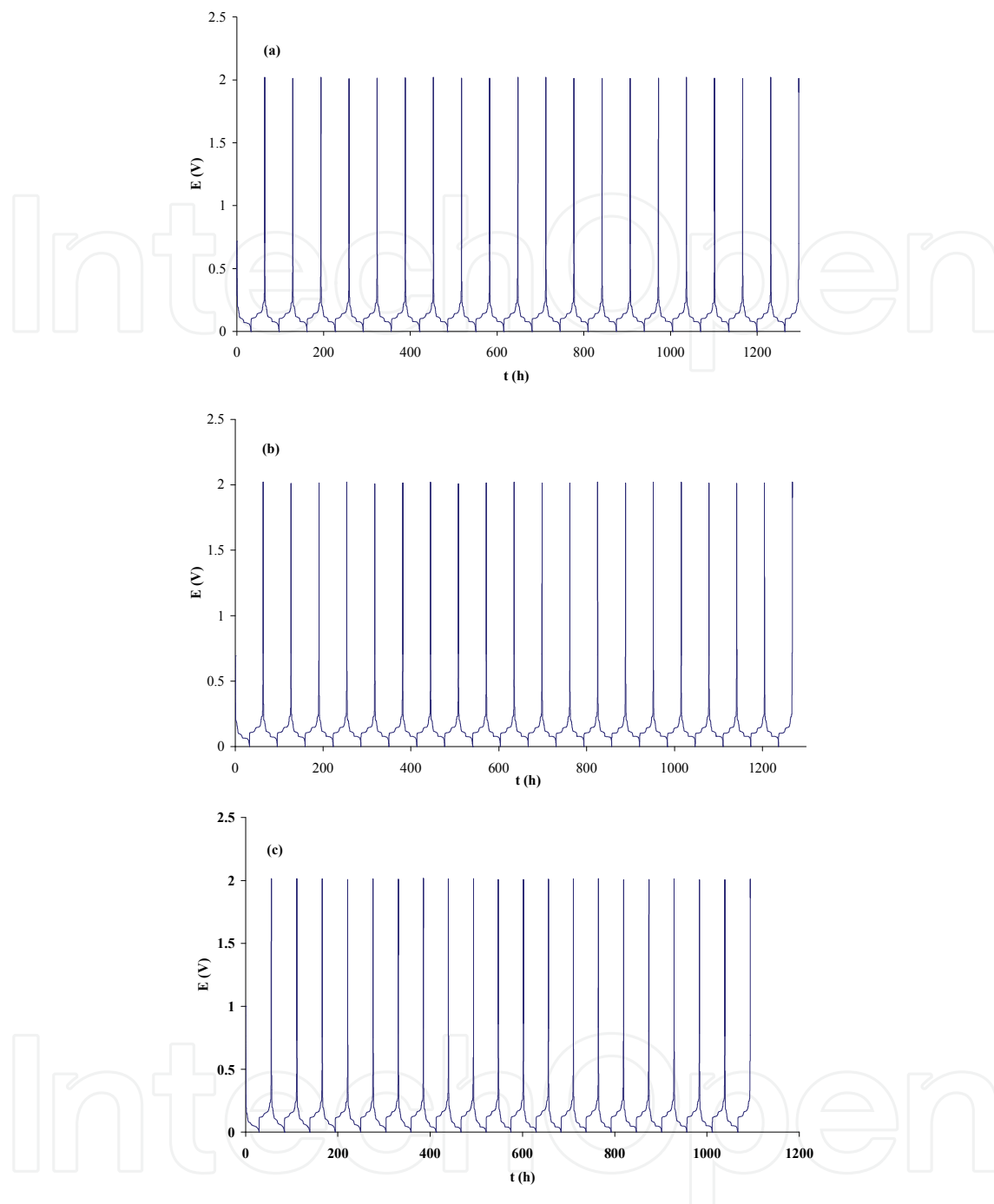


Fig. 16. Galvanostatic chronopotentiometry of a graphite electrode, with an electrolytic solution containing (a) 15 % P₁₅-TFSI, (b) 21 % P₁₅-TFSI and (c) 30 % P₁₅-TFSI; at C/20 and D/20 rates, at 25°C; reference electrode: Li/Li⁺.

All the obtained results are gathered in Table 11. In general, all the tested mixtures give good cycling performances. However the analysis of the cycling of the positive electrode shows that the results depend on the P_{xy}-TFSI RTIL nature, even if no fading or polarisation phenomenon occurs. On one hand, whatever the weight content of P₁₃-TFSI or P₁₄-TFSI is, the resulting capacities do not degrade during the cycling and the standard deviation of the experimental values remains very low (except for the 30% P₁₃-TFSI mixture). On the other

hand, for the mixtures of P₁₅-TFSI and P₂₄-TFSI, RTILs getting the same total number of carbon atoms on both alkyl chains substituting the nitrogen atom, the resulting capacities degrade during the cycling process. This leads to a bigger scattering of the capacity values which are always lower than those obtained with the P₁₃-TFSI or P₁₄-TFSI mixtures. For the graphite electrode, the presence of different plateaus on the chronopotentiometric curves is indicative of good intercalation/de-intercalation processes of the lithium ions. The presence of an electrochemical process occurring the formation of intercalation compounds in the graphite is characteristics of the formation of the SEI layer on the graphite surface. No cycling fading or polarisation phenomenon is observed. Again the negative cycling results are depending on the P_{xy}-TFSI RTIL nature, P₁₄-TFSI giving the best performances and P₁₃-TFSI the worst because of its weaker resistance towards reduction process as expected from linear sweep voltammogram results (Figure 14).

	Positive cycling ability		Negative cycling ability	
	Mean capacity (mA.h.g ⁻¹)	ratio towards the theoretical value (%)	Reversible mean capacity (mA.h.g ⁻¹)	ratio towards the theoretical value (%)
20% P ₁₃ -TFSI	155	97 ± 1	337 ± 14	92 ± 4
20% P ₁₄ -TFSI	159	99 ± 1	354 ± 4	99 ± 1
20% P ₁₅ -TFSI	150	94 ± 3	344 ± 6	95 ± 2
20% P ₂₄ -TFSI	132	83 ± 9	340 ± 19	94 ± 5
30% P ₁₃ -TFSI	150	94 ± 3	268 ± 44	74 ± 12
30% P ₁₄ -TFSI	158	99 ± 1	352 ± 12	97 ± 3
30% P ₁₅ -TFSI	143	89 ± 9	317 ± 16	87 ± 4
30% P ₂₄ -TFSI	130	81 ± 3	309 ± 20	85 ± 5

Table 11. Reversible capacity values of LiCoO₂ and graphite electrodes from cycling in the presence of P_{xy}-TFSI RTIL mixtures at 25°C at C/20 and D/20 rates.

5.3 Conclusion on the electrochemical study

The electrochemical window determination shows that all the studied pyrrolidinium imides can be incorporated in the electrolyte for Li-ion battery except the P₁₃-TFSI RTIL if a graphite electrode is used as negative electrode. These results are confirmed by the galvanostatic chronopotentiometric measurements to test the cycling ability with the electrolyte under consideration. The best electrochemical performances are achieved in the presence of the 20% or 30% P₁₄-TFSI RTIL mixtures

6. General conclusion

To improve the Li-Ion battery security, the use of a series of room temperature ionic liquids is considered. These compounds, abbreviated P_{xy}-TFSI RTILs, consist of a voluminous organic cation of pyrrolidinium-type (P_{xy}⁺) and of the bis(trifluoromethanesulfonyl)imide anion (TFSI⁻). These compounds are not toxic and environmentally friendly because of their very low vapour pressure, which involves a weak volatility. To be compatible with any Li-ion battery applications, an electrolyte has to respect some specifications for thermal, chemical and electrochemical stabilities, for the ionic transport and for electrochemical ability.

The studied P_{xy} -TFSI/standard electrolyte mixtures present a wide temperature range of thermal stability, confirmed by the DSC study and the flammability tests. Even although the mixtures do not really respect the environment, because of the toxicity of the organic solvents and that of the salt of lithium used, the P_{xy} -TFSI RTILs in the mixtures contribute to the improvement of the security of the Li-ion batteries because of their flame-retardant effect. Indeed, the P_{xy} -TFSI co-solvent prevents the most volatile solvent (i.e. DMC) from vaporisation and inflammation, the better protection being achieved from 20% of P_{xy} -TFSI added to the standard electrolyte. The study of the ionic transport properties shows that the mixtures based on 20% of P_{xy} -TFSI are more conductive than the standard electrolyte (except the 20 % P_{15} -TFSI mixture). In the case of P_{14} -TFSI mixtures, when the content is lower than 30%, the resulting conductivity exceeds that of the standard electrolyte. When the content exceeds 30%, the ionic conductivity becomes lower than the standard electrolyte one. However, contents lower than 20% of P_{xy} -TFSI are not of real interest, because the phenomenon of self extinguished flame becomes striking only from 20% of P_{xy} -TFSI. Furthermore, the dynamic viscosity of the standard electrolyte does not vary in a significant way when P_{xy} -TFSI is added as co-solvent, for a content limited to 20% or 30%. Beyond these contents, from 30% to 50%, the increase of the viscosity of mixtures can be a disadvantage for the battery applications at room temperature. All the studied mixtures present a good chemical stability towards the electrode materials. No problem of electrode wetting by the mixtures under consideration is noticed. The use of these mixtures as electrolyte should not raise the problem of wetting, even at low-temperature. The tests of wettability of separators Celgard® (polyolefin type) show a wetting insufficiency. But this problem can be easily resolved by the use of a ceramic type separator such as the Separion®. In addition, the extent of the electrochemical window of the pure P_{xy} -TFSI RTILs is high enough (5.84 V vs. Li/Li⁺), consequently, the electrochemical stability of the mixtures, to introduce them in a Li-ion battery device. In fact, a passivating protected layer is formed at the graphite surface before the lithium ion intercalation processes do occur, that prevents the graphite exfoliation. The galvanostatic chronopotentiometric study on graphite and LiCoO₂ in the presence of mixtures containing 20% or 30% of P_{xy} -TFSI RTILs in the standard electrolyte, gives fairly good results for the electrode cycling ability. However, values of reversible capacity are slightly smaller in the presence of P_{15} -TFSI or of P_{24} -TFSI, than those from tests using P_{13} -TFSI or P_{14} -TFSI RTIL. P_{14} -TFSI gives the best results. Thus, this whole study shows the undeniable contribution a series of N-alkyl-N-alkyl'pyrrolidinium bis(trifluoromethylsulfonyl)imide RTILs in the security of Li-ion batteries, without changing their electrochemical performances.

7. Acknowledgement

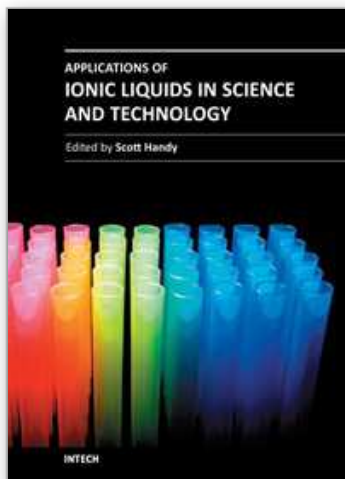
We fully acknowledge the SAFT Company (Bordeaux, France) for its financial support and for having kindly supplied us with electrodes (graphite and LiCoO₂) and with the Separion® separator. We also thank Drs. M. Letellier and P. Porion (CRMD, CNRS-Université d'Orléans, France) for PGSE-NMR measurements, and Pr. D. Lemordant (PCMB, Université François Rabelais, Tours, France) for fruitful discussions.

8. References

- Appetecchi, G. B.; Scaccia, S.; Tizzani, C.; Alessandrini, F. & Passerini, S. (2006). Synthesis of Hydrophobic Ionic Liquids for Electrochemical Applications. *Journal of The Electrochemical Society*, 153, 9, (2006), A1685-A1691

- Appetecchi, G. B.; Kim, G.-T.; Montanino, M.; Alessandrini, F. & Passerini, S. (2008). Solvent-free, PYR14TFSI ionic liquids-based ternary polymer electrolyte systems. II. Battery tests. *ECS Transactions*, 11, 29, (2008, Rechargeable Lithium and Lithium Ion Batteries), 119-129
- Aurbach, D.; Talyosef, Y.; Markovsky, B; Markevich, E.; Zinigrad, E.; Asraf, L.; Gnanaraj, J.S. & Kim, H.J. (2004). Design of electrolyte solutions for Li and Li-ion batteries: a review. *Electrochimica Acta*, 50, 2-3, (2004), 247-254
- Balakrishnan, P.G.; Ramesh, R. & Prem Kumar, T. (2006). Safety mechanisms in lithium-ion batteries. *Journal of Power Sources*, 155, 2, (2006), 401-414
- Cognard, J. (2000) Sciences et Techniques du collage. PPUR, Lausanne, 2000, 26
- Falkenhagen, H. & Vernon, E. L. (1932). The quantitative limiting law for the viscosity of simple strong electrolytes. *Physikalische Zeitschrift*, 33, (1932), 140
- Good, R.J. (1992). Contact angle, wetting and adhesion: a critical review. *Journal of Adhesion Science Technology*, 6, 12, (1992), 1269-1302
- Jones, G. & Dole, M. (1929). The transference number of barium chloride as a function of the concentration. *Journal of the American Chemical Society*, 51, (1929), 1073-1091
- Kaminsky M. (1957). The concentration and temperature dependence of the viscosity of aqueous solutions of strong electrolytes. III. KCl, K₂SO₄, MgCl₂, BeSO₄, and MgSO₄ solutions. *Zeitschrift fuer Physikalische Chemie*, 12, (1957), 206-231
- Kaneko, S.; Kono, Y.; Kobayashi, H.; Ishikawa, H. & Utsuki, K. (2009). Nonaqueous electrolyte solution, gel electrolyte, and secondary lithium battery using the electrolyte solution and the gel electrolyte. *Jpn. Kokai Tokkyo Koho* (2009), JP 2009140641 A 20090625
- Kobayashi, Y.; Mita, Y.; Seki, S.; Ohno, Y.; Miyashiro, H. & Terada, N. (2007). Comparative study of lithium secondary batteries using non-volatile safety electrolytes. *Journal of the Electrochemical Society*, 154, 7, (2007), A677-A681
- Lall-Ramnarine, S.; Castano, A.; Hatcher, J.; Kerr, K.; Li, X.; Munawar, A.; Parikh, A.; Ma, P.; McEntee, C. & Wishart, J. F. (2008). Manipulating the properties of ionic liquids by synthetic design. *Abstracts, 40th Middle Atlantic Regional Meeting of the American Chemical Society*, Queens, NY, United States, May 17-21, (2008), MRM-052
- Lewandowski, A. & Galinski, M. (2004). Carbon-ionic liquid double-layer capacitors. *Journal of Physics and Chemistry of Solids*, 65, 2-3, (2004), 281-286
- MacFarlane, D. R.; Meakin, P.; Sun, J.; A. N. & Forsyth, M. (1999). Pyrrolidinium Imides: A new family of molten salts and conductive plastic crystal phases. *Journal of Physical Chemistry B*, 103, 20, (1999), 4164-4170
- MacNeil, D. D.; Larcher, D. & Dahn, J. R. (1999). Comparison of the reactivity of various carbon electrode materials with electrolyte at elevated temperature. *Journal of the Electrochemical Society*, 146, 10, (1999), 3596-3602
- MacNeil, D. D.; Christensen, L.; Landucci, J.; Paulsen, J. M. & Dahn, J. R. (2000). An autocatalytic mechanism for the reaction of Li_xCoO₂ in electrolyte at elevated temperature. *Journal of the Electrochemical Society*, 147, 3, (2000), 970-979
- MacNeil, D. D. & Dahn, J. R. (2001). Test of reaction kinetics using both differential scanning and accelerating rate calorimetries as applied to the reaction of Li_xCoO₂ in non-aqueous electrolyte. *Journal of Physical Chemistry A*, 105, 18, (2001), 4430-4439
- Martinez, L. M. & Angell, C. A (2001) A thermodynamic connection to the fragility of glass-forming liquids. *Nature*, 410, 6829, (2001), 663-667

- Nockemann, P.; Thijs, B.; Parac-Vogt, T. N.; Van Hecke, K.; Van Meervelt, L.; Tinant, B.; Hartenbach, I.; Schleid, T.; Ngan, V. T. & Nguyen, M. T. (2008). Carboxyl-functionalized task-specific ionic liquids for solubilizing metal oxides. *Inorganic Chemistry*, 47, 21, (2008), 9987-9999
- Pan, Y.; Boyd, L. E.; Kruplak, J. F.; Cleland, W. E., Jr.; Wilkes, J. S. & Hussey, C. L. (2010). Physical and transport properties of bis(trifluoromethylsulfonyl)imide-based room-temperature ionic liquids: Application to the diffusion of tris(2,2'-bipyridyl)ruthenium(II). *Journal of the Electrochemical Society*, 158, 1, (2010), F1-F9
- Papoular, R. J.; Allouchi, H.; Chagnes, A.; Dzyabchenko, A.; Carré, B.; Lemordant, D. & V. Agafonov (2005). X-ray powder diffraction structure determination of γ -butyrolactone at 180 K: phase-problem solution from the lattice energy minimization with two independent molecules. *Acta Crystallographica, Section B:Structural Science*, B61, (2005), 312-320
- Rasch, B.; Cattaneo, E.; Novak, P. & Vielstich, W. (1991). The influence of water on the oxidation of propylene carbonate on platinum. An electrochemical, in-situ FTIR and on-line MS study. *Electrochimica Acta*, 36, 9, (1991), 1397-1402
- Richard, M. N. & Dahn, J. R. (1999). Accelerating rate calorimetry study on the thermal stability of lithium intercalated graphite in electrolyte. I. Experimental. *Journal of the Electrochemical Society*, 146, 6, (1999), 2068-2077
- Shin, J. H. & Cairns, E. J. (2008). Characterization of N-methyl-N-butylpyrrolidinium bis(trifluoromethanesulfonyl)imide-LiTFSI-tetra(ethylene glycol) dimethyl ether mixtures as a Li metal cell electrolyte. *Journal of the Electrochemical Society*, 155, 5, (2008), A368-A373
- Snook, G. A.; Best, A. S.; Pandolfo, A. G. & Hollenkamp, A. F. (2006). Evaluation of a Ag/Ag⁺ reference electrode for use in room temperature ionic liquids. *Electrochemistry Communications*, 8, 9, (2006), 1405-1411
- Stefan, C. S.; Lemordant, D.; Claude-Montigny, B. & Violleau, D. (2009). Are ionic liquids based on pyrrolidinium imide able to wet separators and electrodes used for Li-ion batteries? *Journal of Power Sources*, 189, 2, (2009), 1174-1178
- Stefan, C. S.; Lemordant, D.; Biensan, P.; Siret, C. & Claude-Montigny, B. (2010). Thermal stability and crystallization of N-alkyl-N-alkyl'-pyrrolidinium imides. *Journal of Thermal Analysis and Calorimetry*, 102, 2, (2010), 685-693
- Taggougui, M. (2007). Etudes d'additifs susceptibles de sécuriser les électrolytes des batteries lithium-ion du point de vue : contrôle de charge, de l'effet retardateur de flammes et de la mouillabilité. *Thèse d'Université de Tours*, (12 décembre 2007)
- Wasserscheid, P. & Welton, T. (2008). *Ionic Liquids in Synthesis*. 2008 WILEY-VCH Verlag ISBN 978-3-527-31239-9
- Weast, R. C., (1976). *Handbook of Chemistry and Physics*. 57th Edition (1976-1977) CRC Press
- Xu, W.; Cooper, E. L. & C. Angell, A. (2003a). Ionic Liquids: Ion Mobilities, Glass Temperatures, and Fragilities. *Journal of Physical Chemistry B*, 107, 25, (2003), 6170-6178
- Xu, W.; Wang, L.-M.; Nieman, R. A. & Angell, C. A. (2003b). Ionic Liquids of Chelated Orthoborates as Model Ionic Glassformers. *Journal of Physical Chemistry B*, 107, 42, (2003), 11749-11756
- Zhang, S. S., (2006). A review on electrolyte additives for lithium-ion batteries. *Journal of Power Sources*, 162, 2, (2006), 1379-1394



Applications of Ionic Liquids in Science and Technology

Edited by Prof. Scott Handy

ISBN 978-953-307-605-8

Hard cover, 516 pages

Publisher InTech

Published online 22, September, 2011

Published in print edition September, 2011

This volume, of a two volume set on ionic liquids, focuses on the applications of ionic liquids in a growing range of areas. Throughout the 1990s, it seemed that most of the attention in the area of ionic liquids applications was directed toward their use as solvents for organic and transition-metal-catalyzed reactions. Certainly, this interest continues on to the present date, but the most innovative uses of ionic liquids span a much more diverse field than just synthesis. Some of the main topics of coverage include the application of RTILs in various electronic applications (batteries, capacitors, and light-emitting materials), polymers (synthesis and functionalization), nanomaterials (synthesis and stabilization), and separations. More unusual applications can be noted in the fields of biomass utilization, spectroscopy, optics, lubricants, fuels, and refrigerants. It is hoped that the diversity of this volume will serve as an inspiration for even further advances in the use of RTILs.

How to reference

In order to correctly reference this scholarly work, feel free to copy and paste the following:

Claude-Montigny Bénédicte, Stefan Claudia Simona and Violleau David (2011). Undeniable Contribution of Aprotic Room Temperature Ionic Liquids in the Security of Li-Ion Batteries, Applications of Ionic Liquids in Science and Technology, Prof. Scott Handy (Ed.), ISBN: 978-953-307-605-8, InTech, Available from: <http://www.intechopen.com/books/applications-of-ionic-liquids-in-science-and-technology/undeniable-contribution-of-aprotic-room-temperature-ionic-liquids-in-the-security-of-li-ion-batterie>

INTECH
open science | open minds

InTech Europe

University Campus STeP Ri
Slavka Krautzeka 83/A
51000 Rijeka, Croatia
Phone: +385 (51) 770 447
Fax: +385 (51) 686 166
www.intechopen.com

InTech China

Unit 405, Office Block, Hotel Equatorial Shanghai
No.65, Yan An Road (West), Shanghai, 200040, China
中国上海市延安西路65号上海国际贵都大饭店办公楼405单元
Phone: +86-21-62489820
Fax: +86-21-62489821

© 2011 The Author(s). Licensee IntechOpen. This chapter is distributed under the terms of the [Creative Commons Attribution-NonCommercial-ShareAlike-3.0 License](#), which permits use, distribution and reproduction for non-commercial purposes, provided the original is properly cited and derivative works building on this content are distributed under the same license.

IntechOpen

IntechOpen